Improved Neuronal Tract Tracing with Stable Biocytin-Derived Neuroimaging Agents

Anurag Mishra,*[,†,‡] Kirti Dhingra,[†] Almut Schüz,[†] Nikos K. Logothetis,[†,§] and Santiago Canals*[,†,⊥]

[†]Department for Physiology of Cognitive Processes, Max Planck Institute for Biological Cybernetics, Spemannstrasse 38, Tübingen 72076, Germany, and [§]Imaging Science and Biomedical Engineering, University of Manchester, Manchester M13 9PL, U.K.

Abstract

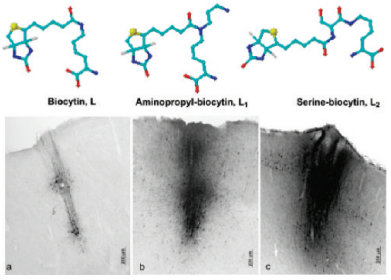

One of the main characteristics of brains is their profuse connectivity at different spatial scales. Understanding brain function evidently first requires a comprehensive description of neuronal anatomical connections. Not surprisingly a large number of histological markers were developed over the years that can be used for tracing mono- or polysynaptic connections. Biocytin is a classical neuroanatomical tracer commonly used to map brain connectivity. However, the endogenous degradation of the molecule by the action of biotinidase enzymes precludes its applicability in long-term experiments and limits the quality and completeness of the rendered connections. With the aim to improve the stability of this classical tracer, two novel biocytin-derived compounds were designed and synthesized. Here we present their greatly improved stability in biological tissue along with retained capacity to function as neuronal tracers. The experiments, 24 and 96 h postinjection, demonstrated that the newly synthesized molecules yielded more detailed and complete information about brain networks than that obtained with conventional biocytin. Preliminary results suggest that the reported molecular designs can be further diversified for use as multimodal tracers in combined MRI and optical or electron microscopy experiments.

Keywords: Brain mapping, neuroanatomical tracers, biocytin, biotinidase, histology

Biocytin is a classical neuroanatomical tracer that has been successfully applied in brain connectivity studies. It is efficiently taken up by neurons and transported in both anterograde and retrograde direction (*1*−*3*). Several characteristics make biocytin an excellent tracer; hence it is extensively used in neuroanatomical research employing histochemical techniques (*3*−*5*), after either intra- or extracellular application. Due to its high affinity for avidin, biocytin can be visualized by using a host of avidin-conjugated markers at the light and electron microscopic level (*2*, *5*, *6*). Several studies have been reported where biocytin was used to visualize the morphology of dendritic and axonal arborizations (*7*−*15*).

Structurally, biocytin is a conjugate of D-biotin and L-lysine, where the carboxylate of D-biotin is coupled with the ϵ-amine of L-lysine via a secondary amide bond(*16*) (Figure 1). The main drawback associated with biocytin is its relatively short half-life *in vivo* due to the rapid cleavage of the secondary amide in the presence of biotinidase, an enzyme present in biological tissues. Degradation of biocytin by biotinidase begins a few hours after application (*17*−*19*). The instability of biocytin makes it inappropriate for use as neuronal tract tracer in experiments with long postinjection survival times. This disadvantage forces short postinjection incubation times and, thus, increases the probability of partial reconstruction of neuronal connections at the network level or the incomplete reconstruction of axonal arbors at the cellular level (*1*, *4*, *6*). Therefore, improving the postinjection lifetime of biocytin could considerably contribute to the visualization of anatomical connections and provide valuable information on the afferent and efferent connectivity of the brain.

Synthetically, few strategies have been formulated to improve the stability of biotinylated molecules, including the use of sterically hindered amide bonds (such as *tert*-amide or α-carboxylate/hydroxyl/amide) to render the linkage stable against biotinadase (*20*, *21*). By the same strategy, two new biocytin-based tracers [aminopropyl-biocytin (**L_1**) and serine-biocytin (**L_2**); Figure 1)] have been designed. The first tracer, **L_1**, includes propylamine on an amide linkage of biocytin to obtain a stable *tert*-amide construct. Another tracer, **L_2**, is serine-based, where amine and carboxylate functional moieties of serine are connected via amide

Received Date: August 28, 2009
Accepted Date: September 20, 2009
Published on Web Date: October 06, 2009

DOI: 10.1021/cn900010d | *ACS Chem. Neurosci.* (2010), *1*, 129–138

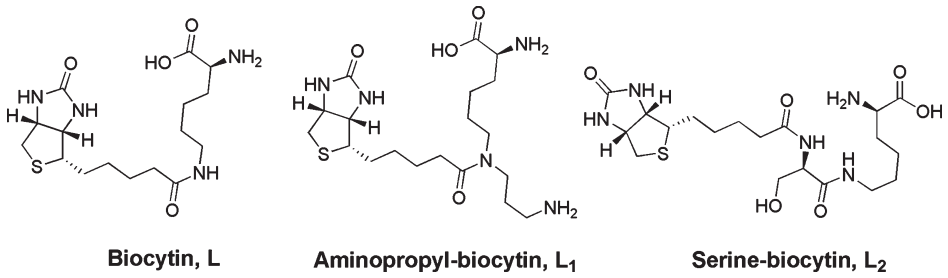

Figure 1. Studied biocytin derivatives as neuroanatomical tract tracers.

Scheme 1[a]

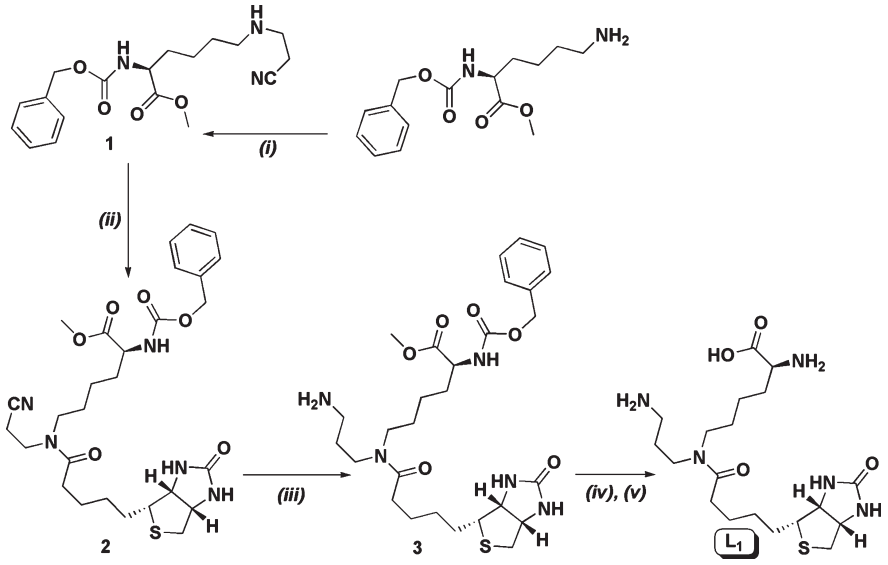

[a] Reagents and conditions: (i) acrylonitrile, TEA, MeOH; (ii) D-biotin, PyBroP, DIPEA, dry CH_2Cl_2; (iii) Ra-Ni, H_2, 7 M NH_3/MeOH, 50 psi; (iv) Pd−C (10%), H_2, MeOH, 50 psi; (v) LiOH, THF/MeOH/water (3:2:2).

linkage with biotin and the ε-amine of L-lysine respectively. We performed a series of neuroanatomical investigations to test $\mathbf{L_1}$ and $\mathbf{L_2}$ compounds and contrast their tracing capabilities with a standard (commercial) biocytin molecule. Our results demonstrate that (i) the stability of the newly synthesized compounds in brain tissue is greatly improved, (ii) the molecules retain full tracing capabilities, and more importantly, (iii) due to the improved stability, these molecules allow longer postinjection survival times and, therefore, provide more detailed and complete connectivity information.

Results and Discussion

Synthesis of Tracers

The first tracer, aminopropyl-biocytin ($\mathbf{L_1}$), was synthesized in five steps, starting with reaction of acrylonitrile on $^{\alpha}$*N*-carbobenzyloxy-L-lysine methyl ester giving compound **1**. Propiononitrile-including biocytin, **2**, was obtained after coupling of the carboxylate of D-biotin with the secondary amine of **1** by using dry CH_2Cl_2 as solvent, PyBroP as coupling reagent, and diisopropylethylamine as base. The selective reduction of the nitrile group in the presence of Ra-Ni, H_2, and 7 M NH_3/MeOH yielded amine **3**. The removal of the $^{\alpha}$*N*-carbobenzyloxy group by Pd−C (10%), H_2, and MeOH and deprotection of the methyl group by LiOH and THF/MeOH/water (3:2:2) gave $\mathbf{L_1}$ (Scheme 1).

The synthesis of the second tracer, serine-biocytin ($\mathbf{L_2}$), was carried out according to Scheme 2. The primary alcoholic group in *N*-carbobenzyloxy-L-serine methyl ester was protected with TBDMS to give **4**. The hydrolysis of methyl ester in **4** was carried out with LiOH to obtain compound **5**. The lysine precursor was synthesized from Boc-Lys-(*Z*)-OH by first esterifying the carboxylate group with MeOH/DCC to get **6** and then removing the Cbz protecting group to get amine **7** (*22*). To obtain the intermediate product **8**, the amine of **7** was coupled to the carboxylate of **5** via an amide bond using EDC/HOBt/NMM as the coupling reagents. The TBDMS group in **8** was removed with TBAF to get the free alcohol in **9**. The primary alcoholic group was then reprotected with isobutyl chloroformate to give **10**.

DOI: 10.1021/cn900010d | ACS Chem. Neurosci. (2010), 1, 129–138

Scheme 2 [a]

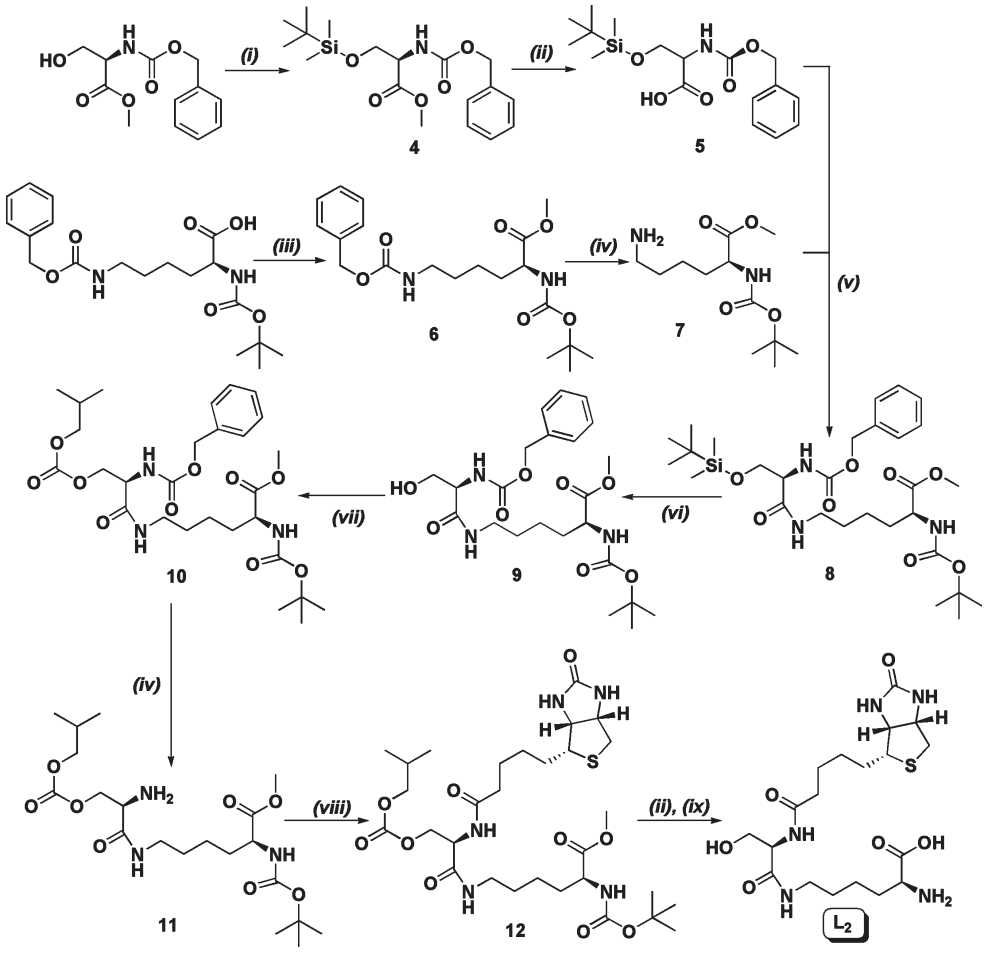

[a] Reagents and conditions: (i) TBDMS-Cl/imidazole/DMF; (ii) LiOH−THF/MeOH/H_2O (3:2:2); (iii) MeOH/DCC/CH_2Cl_2; (iv) Pd−C (10%), H_2, MeOH, 50 psi; (v) EDC/NMM/HOBt/DMF; (vi) TBAF/THF; (vii) *i*-Bu-chloroformate/pyridine/CH_2Cl_2; (viii) HATU/DIPEA/DMF; (ix) TFA/CH_2Cl_2.

The CBz group in **10** was removed, which yielded the amine **11**. The amine moiety of **11** was coupled to carboxylate of D-biotin via amide bond to give protected serine biocytin, **12**. Finally, the hydrolysis of the methyl ester in **12** under basic condition and Boc/isobutyl carbonate hydrolysis under acidic conditions using neat TFA at room temperature yielded the final product serine-biocytin, $\mathbf{L_2}$. The deprotection of the TBDMS group in **8** and then reprotection in **9** by isobutyl chloroformate to get **10** was carried out because removal of TBDMS at the last stage with TBAF yielded the product with some impurities from the TBAF reagent. The impurities and the final product both being soluble in water made the purification of product difficult. To avoid the extra protection and deprotection steps, we started by protecting the alcohol group on *N*-carbobenzyloxy-L-serine methyl ester with isobutyl chloroformate. However, in the next step the hydrolysis of the methyl ester with LiOH removed the isobutyl carbonate group because of its instability to the carboxylate formed after the hydrolysis of the methyl ester in the molecule.

Both modified compounds are structurally similar to the conventional biocytin having D-biotin and the α-position of L-lysine moieties free to keep them active as potential tracers. However, the linkage between lysine and biotin being sterically hindered makes these new agents more stable than conventional biocytin. The first molecule has an additional amine moiety, and the second one has an α-hydroxyl group, which provides better solubility in physiological buffers compared with that reported for biocytin. Interestingly, these molecular designs allow the attachment of additional functional groups as fluorophores or macrocycles carrying paramagnetic metal ions, paving the way to a new generation of multimodal neuroanatomical tracers for MRI-based *in vivo* tracing studies and fluorescence optical imaging.

Comparative Histological Studies of L, L_1, and L_2 after Iontophoretic Injections in the Brain

To evaluate whether the newly synthesized biocytin derivatives $\mathbf{L_1}$ and $\mathbf{L_2}$ maintained similar tracing abilities and with higher stability under *in vivo* conditions than

DOI: 10.1021/cn900010d | *ACS Chem. Neurosci.* (2010), *1*, 129–138

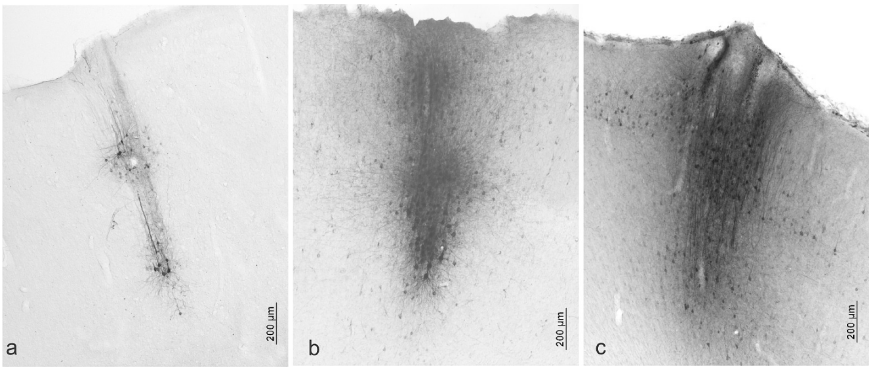

Figure 2. Comparative histological studies of **L** (a), $\mathbf{L_1}$ (b), and $\mathbf{L_2}$ (c) showing the injection site in the cerebral cortex of a rat after a survival time of 24 h. The higher stability of $\mathbf{L_1}$ and $\mathbf{L_2}$ compared with **L** is visible already after 24 h.

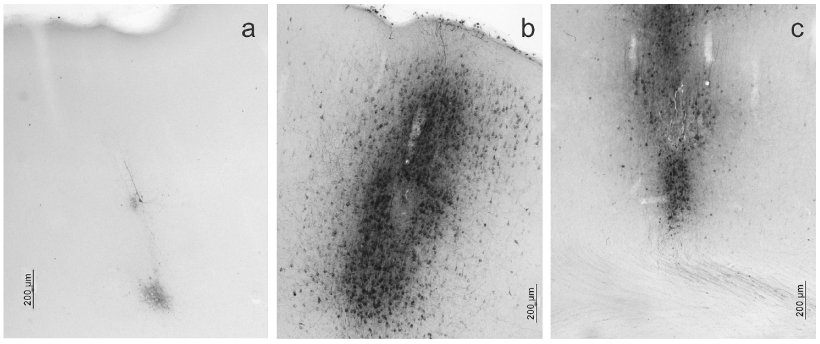

Figure 3. Comparison of **L** (a), $\mathbf{L_1}$ (b), and $\mathbf{L_2}$ (c) in the cerebral cortex of the rat after a survival time of 96 h. The injection site of **L** is hardly visible, while the injection sites of $\mathbf{L_1}$ and $\mathbf{L_2}$ do not differ in intensity from those after 24 h.

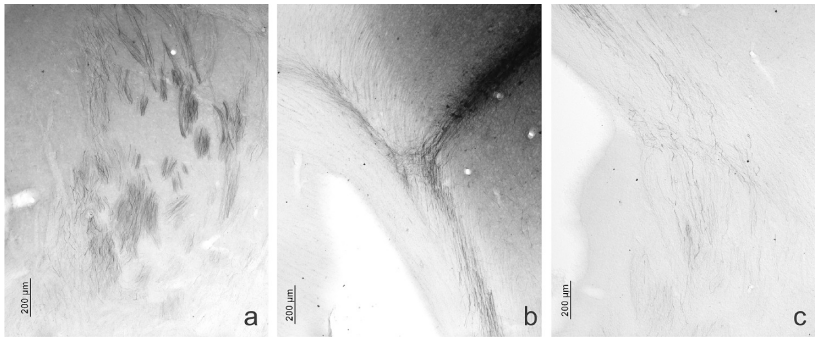

Figure 4. Comparison of **L** (a) and $\mathbf{L_1}$ (b, c) after 1 h survival time in the rat brain: (a) axon bundles in the striatum; (b) axons in the white matter emanating from the injection site; (c) same animal, showing axons in the striatum. Both tracers show equally good uptake and transport after 1 h.

conventional biocytin (**L**), we performed a series of iontophoretic injections into the primary motor cortex of anaesthetized albino rats (Sprague−Dawley) and compared the neuronal uptake and transport of the three compounds, as well as the intensity of the stain at 24 and 96 h of survival time. All injections were performed with the same starting concentration of tracer molecules (4%), the same iontophoretic parameters, and comparable pipet tip diameter and impedance (see Experimental Methods) to ensure an equivalent application of all compounds. As shown in Figure 2, both new molecules were efficiently taken up at the injection site. The figure also shows that after 24 h the intensity of the histological staining reflecting the amount of non-degraded molecule (or molecule with intact avidin binding capacity) was clearly higher for the new modified tracers ($\mathbf{L_1}$ and $\mathbf{L_2}$) than for the conventional biocytin (**L**). As expected, this effect was more striking when the survival time, and thus the time of exposure to endogenous biotinidase activity, was increased to 96 h (Figure 3). In order to prove that the weaker stain obtained with conventional biocytin in Figures 2 and 3 is indeed due to its lower stability and not to differences during the iontophoretic application; we also performed

DOI: 10.1021/cn900010d | ACS Chem. Neurosci. (2010), 1, 129–138

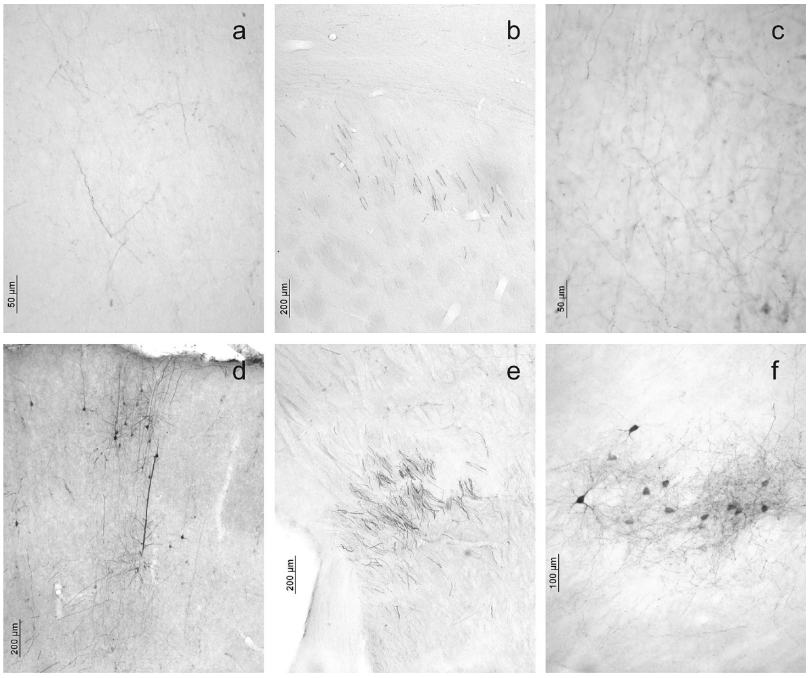

Figure 5. Examples of anterograde or retrograde transport of **L** (a, b), of $\mathbf{L_1}$ (c), and of $\mathbf{L_2}$ (d−f) after injection into the primary motor cortex and a survival time of 24 h. (a, c) axon terminals in the contralateral hemisphere; (b, e) axons running through the striatum; (d) retrogradely stained neurons in a different cortical area; (f) retrogradely stained neurons in the thalamus.

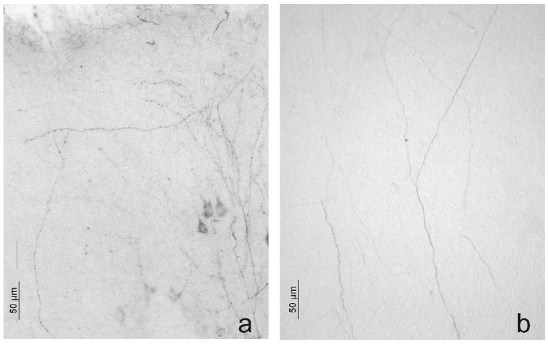

Figure 6. Transport of $\mathbf{L_1}$ (a) and of $\mathbf{L_2}$ (b) after a survival time of 96 h: (a) anterogradely stained ascending axons and some retrogradely stained neurons in the ipsilateral cortex; (b) ascending axons in the contralateral hemisphere.

experiments on **L** and $\mathbf{L_1}$ with only 1 h survival time (Figure 4). After such a short survival time, there was no detectable difference in the size of the injection site or in the degree of neuronal uptake. In addition, by 1 h, the transport of regular or modified biocytin molecules had occurred already down into the striatum, indicating that the prominent tracings seen at long postinjection times with compounds $\mathbf{L_1}$ and $\mathbf{L_2}$ directly reflect an increase in the stability of the molecules rather than an improvement in the efficiency of transport itself. Some examples of tract tracing with $\mathbf{L_1}$ and $\mathbf{L_2}$ visualizing connections of the primary motor cortex of the rat are shown in Figures 5 and 6.

Most significantly, labeled fibers far from the injection site were seen after 96 h postinjection time with the modified tracers (Figure 6) but were not observed with the conventional variant. At this postinjection time, commercial biocytin failed to show detectable transport even in the vicinity of the injection site (where most of the stained material is located). These results clearly demonstrate that the reported modification of biocytin conferred stability to the molecules and increased their applicability as neuronal tract tracer.

Conclusion

In summary, the new stable tracing agents ($\mathbf{L_1}$ and $\mathbf{L_2}$) were designed and synthesized, and an assessment of their uptake and transport ability by commonly used histochemical procedures was performed. The linking of biotin and lysine moieties in both molecules were performed in such a way that the new molecules are resistant to cleavage by the action of biotinidase. The *in vivo* experiments performed on these synthesized derivatives of biocytin proved that they are indeed more stable conjugates. The staining of neuronal cell bodies and fibers at the injection site and remote terminal fields were retained even at 96 h postinjection times, when commercial biocytin was nearly degraded. Anterograde or retrograde transport could be found in the ipsi- and contralateral cortex, striatum, thalamus, and further down in the brain stem, demonstrating their efficient

DOI: 10.1021/cn900010d | *ACS Chem. Neurosci.* (2010), *1*, 129–138

transport along axons. Thus $\mathbf{L_1}$ and $\mathbf{L_2}$ represent an excellent alternative for conventional histological studies that would alleviate the problems caused by the endogenous degradation of the tracer molecule before the animal is sacrificed. Importantly, the molecular design of these agents could be easily diversified for use as multimodal tracers after coupling different reporter moieties. Thus, the reported molecules could serve as a potent tool for the development of agents that can be visualized with magnetic resonance imaging and thus be used for the *in vivo* study of brain connectivity.

Experimental Methods

Chemicals

All solvents and reagents were used at the purest grade commercially available without further purification. D-Biotin, *N*-methylmorpholine (NMM), 1-hydroxybenzotriazole hydrate (HOBt), *N*′-(3-dimethylaminopropyl)-*N*-ethylcarbodiimide hydrochloride (EDC), dicyclohexylcarbodiimide (DCC), *tert*-butyldimethylsilylchloride (TBDMS-Cl), isobutylchloroformate, *O*-(7-azabenzotriazol-1-yl)-*N*,*N*,*N*′,*N*′-tetramethyluronium hexafluorophosphate (HATU), imidazole, tetrabutylammonium fluoride (TBAF), *N*,*N*-dimethylformamide (DMF extra dry), palladium on carbon (Pd−C, 10%), acrylonitrile, $^{\alpha}$*N*-carbobenzyloxy-L-lysine methyl ester, *N*-carbobenzyloxy-L-serine methyl ester, *N*,*N*-diisopropylethylamine (DIPEA), bromotripyrrolidinophosphonium hexafluorophosphate (PyBroP), and lithium hydroxide were purchased from Aldrich, Germany. Methanol, dichloromethane, *n*-hexane, ethyl acetate (EtOAc), acetonitrile (MeCN, HPLC grade), silica gel 60 (70−230 mesh), tetrahydrofuran (THF), triethylamine (TEA), sodium sulfate, Raney nickel (Ra-Ni), 7 M ammonia in methanol (NH_3/MeOH), lithium hydroxide (LiOH), trifluoroacetic acid (TFA), and pyridine were purchased from Fluka, Germany. Pure water (18 MΩ cm^{-1}) was used throughout.

Reverse-Phase High-Performance Liquid Chromatography (RP-HPLC)

RP-HPLC was performed at room temperature on a Varian PrepStar Instrument, Australia, equipped with PrepStar SD-1 pump heads. UV absorbance was measured using a ProStar 335 photodiode array detector at 214 and 254 nm. Analytical RP-HPLC was performed in a stainless steel Chromsep (length 250 mm, internal diameter 4.6 mm, outside diameter 3/8 in., and particle size 8 μm) C_{18} column, and semipreparative RP-HPLC was performed on a stainless steel Chromsep (length 250 mm, internal diameter 21.2 mm, and particle size 5 μm) C_{18} column (Varian, Advanced Chromatographic Solutions). The compounds were purified using one of two methods. Method A involved a gradient with the mobile phase starting from 95% solvent A (H_2O, 0.05% TFA) and 5% of solvent B (acetonitrile, 0.05% TFA) to 70% B in 10 min, 90% B in 18 min, 90% B isocratic until 24 min, and decrease to 5% B in 28 min. Alternatively, method B involved 95% solvent A (H_2O, 0.1% HCOOH) and 5% solvent B (acetonitrile, 0.1% HCOOH) to 70% solvent B in 10 min and then to 100% in next 8 min running isocratic for 12 min after that and then back to 5% solvent B in next 2 min. The flow rate used for analytical HPLC was 1 mL/min and for semipreparative HPLC was 15 mL/min. All the solvents for HPLC were filtered through a nylon-66 Millipore filter (0.45 μm) prior to use.

Spectroscopy

^{1}H NMR and ^{13}C NMR spectra were recorded on Bruker DRX250 and DRX400 spectrometers at room temperature. The ^{1}H NMR chemical shifts were adjusted to the residual protons of the solvent peaks, which were referenced to TMS (0.00 ppm), and ^{13}C NMR chemical shifts were referenced to $CDCl_3$ (77.0 ppm). Mass spectra (ESI-MS in positive and negative ion mode) were performed on an ion trap SL 1100 system (Agilent, Germany) and ESI-HRMS on Bruker Daltonics Apex II FT-ICR-MS (Bruker, Germany).

In Vivo Rat Experiments

To test whether the newly designed tracers, $\mathbf{L_1}$ and $\mathbf{L_2}$, were more stable *in vivo* than conventional biocytin (**L**), we performed iontophoretic injections of all three compounds into the cortex of 10 albino rats (Sprague−Dawley). Five rats (two with **L**, one with $\mathbf{L_1}$, and two with $\mathbf{L_2}$) were sacrificed after a survival time of 24 h, three rats (with **L**, $\mathbf{L_1}$, and $\mathbf{L_2}$) after a survival time of 96 h, and two rats (with **L** and $\mathbf{L_1}$) after 1 h.

Injections

All rats were anaesthetized with 2% isoflurane (Abbott). One compound per animal was injected into the primary motor cortex at two or three different levels. In the animals with a survival time of 24 h, two injections were made, at depths of 250 and 500 μm. In the case of the animals with a survival time of 96 h, a third injection was made at a depth of 750 μm.

Borosilicate pipettes with tip diameter of 20 μm were used for iontophoresis. Each injection was made over a period of 30 min (7 s on, 7 s off) with 10 μA current (except in the case of the animals shown in Figure 1 where we used 5 μA).

At the end of the procedure, the animals received an intraperitoneal injection of analgesics and antibiotics [5 mg/kg Baytril (Bayer) and 2.5 mg/kg Finadyne (Essex)]. The animals with a survival time of 96 h received another injection of these substances after 24 h.

Perfusion

After 1, 24, and 96 h, the animals were anaesthetized again with isoflurane and received a lethal intraperitoneal injection of the barbiturate pentobarbital sodium (Narcoren from Merial; 2.5 mL/kg of body weight). After cessation of all reflexes, the chest of the animal was opened, and 0.4 mL of heparin-sodium 25000 (Ratiopharm) was injected into the heart in order to prevent coagulation. Then a canule was inserted, and the animal was perfused with isotonic saline (using NaCl 0.9 E from Fresenius) for about 5 min and then with the fixative (commercially available 4% paraformaldehyde, phosphate-buffered; Roti-Histofix 4% from Carl Roth, No. P087.3).

The brain was removed from the skull and kept in the fixative media overnight. On the next day, the brain was transferred into 30% sucrose in demineralized water and kept there for at least 4 days until it had sunk. The brain was then cut with a freezing microtome into serial sections at a thickness of 70 μm.

DOI: 10.1021/cn900010d | *ACS Chem. Neurosci.* (2010), *1*, 129–138

Histological Procedure

The protocol followed largely that of Horikawa and Armstrong, (*5*) with some modifications suggested by Dr. Michaela Schweizer (personal communication). In detail, the sections were collected in phosphate buffer (PB, 0.1 M; pH 7.3), rinsed again in PB, and then transferred into 1% H_2O_2 in PB for 1 h in order to suppress endogenous peroxidase activity. After being rinsed 3 times in PB, the sections were kept for 1 h in Triton X-100 (Carl Roth; 2% in 0.1 M PB). They were then incubated overnight in avidin-conjugated peroxidase, using an ABC Elite PK 6100 (Linaris, 1% in 0.1 M PB; that is, 10 drops at 50 μL of each of the two solutions to 49 mL of PB. Note that the ABC mixture must be allowed to stand for 30 min before use). On the next day, the sections were rinsed 2 × 10 min in PB (0.1 M) and then 2 × 10 min in Tris/HCl at pH 7.9 (using a 0.1 M solution of tris-(hydroxymethyl)-aminomethane from Carl Roth, No. 5429.1, or Merck, molecular weight M = 121.14 g/mol, and adjusting the pH to 7.9 with HCl; we usually used a 1 M stem cell solution, the pH of which we adjusted with concentrated HCl). Then the sections were transferred into a solution of diamino benzidine and H_2O_2 (DAB, Sigma fast tablet set, D-4293, dissolved in demineralized water) for 30−45 min. After being washed 3 times in Tris/HCl, the sections were transferred into 0.05 M phosphate buffer and mounted on electrostatical slides (Superfrost Plus, Menzel, Thermo-Scientific), air-dried overnight, dehydrated in ethanol (70%, 80%, 2 × 99%, 2 × 100% ethanol, 2 × terpineole, and 2 × xylene), and covered in Eukitt or DePeX.

Synthesis of Tracers

(*S*)-Methyl 2-(Benzyloxycarbonylamino)-6-(2-cyanoethylamino)hexanoate (1). A solution of $^{\alpha}$*N*-carbobenzyloxy-L-lysine methyl ester (2 g, 6.8 mmol), TEA (1.9 mL, 13.6 mmol), and acrylonitrile (0.9 mL, 13.6 mmol) in 20 mL of MeOH was stirred at room temperature for 18 h. The reaction progress was monitored by thin layer chromatography (TLC). TLC was run on aluminum sheet silica gel plates with 0.2 mm thick silica gel 60 F_{254} (E. Merck, Germany) using DCM/MeOH, 9.5:0.5, as the mobile phase. The TLC plate was developed in an iodine chamber, and the R_f of **1** was 0.6. After completion, the solvent was evaporated under reduced pressure, and the compound was purified by column chromatography (silica gel, 5% MeOH in CH_2Cl_2) to give 1.8 g (75%) of **1** as a yellowish gum residue. ^{1}H NMR ($CDCl_3$, 250 MHz), δ (ppm): 1.25−1.34 (m, 2H); 1.36−1.46 (m, 2H); 1.54−1.64 (m, 2H); 1.70−1.82 (m, 1H); 2.40 (t, J = 6.66 Hz, 2H); 2.53 (t, J = 6.87 Hz, 2H); 2.80 (t, J = 6.62 Hz, 2H); 3.66 (s, 3H); 4.26−4.31 (m, 1H); 5.03 (s, 2H); 5.43−5.52 (m, 1H); 7.21−7.3 (m, 5H). ^{13}C NMR ($CDCl_3$, 62.9 MHz), δ (ppm): 18.2; 22.4; 28.9; 31.9; 44.6; 48.3; 52.0; 53.4; 66.6; 118.4; 127.7; 127.9; 128.2; 135.9; 155.6; 172.6. ESI-HRMS (+): calcd $C_{18}H_{25}N_3O_4$ m/z 348.1917 $(M + H)^+$; found 348.1917 $(M + H)^+$.

(*S*)-Methyl 2-(Benzyloxycarbonylamino)-6-(*N*-(2-cyanoethyl)-5-((3a*R*,4*R*,6a*S*)-2-oxo-hexahydro-1*H*-thieno[3,4-*d*]-imidazol-4-yl)pentanamido)hexanoate (2). A solution of **1** (1.5 g, 4.3 mmol), D-biotin (1.16 g, 4.8 mmol), DIPEA (0.18 mL, 1.7 mmol), and PyBroP (4.03 g, 8.6 mmol) in CH_2Cl_2 (50 mL) was stirred overnight at room temperature. The reaction progress was monitored by TLC using CH_2Cl_2/MeOH, 9:1, and the R_f of **2** was 0.45. After completion, the reaction mixture was poured into water and extracted with CH_2Cl_2 (3 × 100 mL); organic layer was dried over anhydrous Na_2SO_4 and filtered, and the filtrate was evaporated under reduced pressure and purified by column chromatography (silica gel, 10% MeOH in CH_2Cl_2) to give 1.54 g (62%) of **2** as off-white solid. ^{1}H NMR ($CDCl_3$, 250 MHz), δ (ppm): 1.18−1.39 (m, 4H); 1.42−1.80 (m, 8H); 2.25 (t, J = 6.64 Hz, 2H); 2.58 (t, J = 6.62 Hz, 2H); 2.51−2.55 (m, 1H); 2.74−2.82 (m, 1H); 3.00−3.11 (m, 1H); 3.26 (t, J = 6.72 Hz, 2H); 3.37−3.53 (m, 2H); 3.67 (s, 3H); 4.14−4.22 (m, 1H); 4.25−4.32 (m, 1H); 4.34−4.41 (m, 1H); 5.04 (s, 2H); 5.67 (br s, 1H); 5.77−5.93 (m, 1H); 6.15 (br s, 1H); 7.21−7.31 (m, 5H). ^{13}C NMR ($CDCl_3$, 62.9 MHz), δ (ppm): 16.2; 22.5; 24.9; 28.1; 28.3; 28.5; 32.0; 32.4; 40.4; 42.6; 48.9; 52.4; 53.5; 55.4; 60.1; 61.8; 66.9; 118.4; 127.9; 128.1; 128.4; 136.2; 156.0; 163.9; 172.9; 173.4. ESI-HRMS (+): calcd $C_{28}H_{39}N_5O_6S$ m/z 574.2693 $(M + H)^+$; found 574.2700 $(M + H)^+$.

(*S*)-Methyl 6-(*N*-(3-Aminopropyl)-5-((3a*R*,4*R*,6a*S*)-2-oxo-hexahydro-1*H*-thieno[3,4-*d*]imidazol-4-yl)pentanamido)-2-(benzyloxycarbonylamino)hexanoate (3). A solution of **2** (0.8 g, 1.4 mmol), activated Ra-Ni (0.2 g w/w), and H_2 (50 psi) in 7 M NH_3/MeOH (20 mL) was stirred at room temperature in a Parr apparatus for 6 h. The progress of the reaction was monitored by ESI-MS. After completion, the solvent was evaporated under reduced pressure, and the residue was purified by preparative RP-HPLC {method A, λ = 214 nm, retention time (RT) = 11.2 min}. After lyophilization, 0.56 g (70%) of **3** as off-white solid was obtained. ^{1}H NMR ($CDCl_3$, 250 MHz), δ (ppm): 1.08−1.98 (m, 15H); 2.24 (br s, 2H); 2.47−3.44 (m, 8H); 3.65 (s, 3H); 3.88−4.59 (m, 3H); 5.01 (s, 2H); 5.66−6.37 (m, 1H); 6.39−7.00 (m, 1H); 7.16−7.33 (m, 5H); 8.02 (br s, 3H). ^{13}C NMR ($CDCl_3$, 62.9 MHz), δ (ppm): 22.2; 24.9; 25.6; 27.3; 27.8; 28.4; 31.0; 32.2; 36.8; 39.7; 42.2; 45.0; 47.4; 47.7; 49.4; 52.7; 55.3; 60.2; 62.1; 66.6; 127.5; 128.1; 128.5; 136.3; 157.2; 165.1; 174.2; 175.7. ESI-HRMS (+): calcd $C_{28}H_{43}N_5O_6S$ m/z 578.3006 $(M + H)^+$; found 578.3010 $(M + H)^+$.

(*S*)-2-Amino-6-(*N*-(3-aminopropyl)-5-((3a*S*,4*S*,6a*R*)-2-oxo-hexahydro-1*H*-thieno[3,4-*d*]imidazol-4-yl)pentanamido)hexanoic Acid (Aminopropyl-biocytin, L_1). A solution of **3** (0.09 g, 0.16 mmol), 10% Pd−C (0.03 g, w/w), and H_2 (50 psi) in MeOH (10 mL) was stirred at room temperature in Parr apparatus for 6 h. The reaction was monitored by ESI-MS. After completion, the reaction mixture was filtered through a G-4 sintered funnel; filtrate was evaporated under reduced pressure. This crude product was dissolved in 20 mL of THF/MeOH/water (3:2:2) and stirred at 0−5 °C for 15 min, and then LiOH (0.11 g, 4.7 mmol) was added. The reaction mixture was stirred for 2 h at room temperature. The progress of the reaction was monitored by ESI-MS. After completion, the pH was adjusted to 7 with HCOOH, and solvent was evaporated under reduced pressure. Finally, the residue was purified by preparative HPLC (method A, λ = 214 nm, RT = 8.2 min). After lyophilization, 78% of tracer $\mathbf{L_1}$ as an off-white solid compound was obtained. ^{1}H NMR (D_2O, 250 MHz), δ (ppm): 1.40−1.86 (m, 10H); 1.93−2.15 (m, 4H); 2.53 (t, J = 7.02 Hz, 2H); 2.81−2.90 (m, 1H);

DOI: 10.1021/cn900010d | ACS Chem. Neurosci. (2010), 1, 129–138

2.98−3.16 (m, 3H); 3.38−3.60 (m, 5H); 4.15−4.25 (m, 1H); 4.46−4.54 (m, 1H); 4.66−4.72 (m, 1H). ^{13}C NMR (D_2O, 62.9 MHz), δ (ppm): 27.2; 27.3; 38.0; 48.5; 48.8; 49.1; 49.6; 52.9; 54.9; 55.1; 81.3; 81.5; 171.5; 171.9. ESI-HRMS (+): calcd $C_{19}H_{35}N_5O_4S$ m/z 430.2482 $(M + H)^+$; found 430.2480 $(M + H)^+$.

(*R*)-Methyl 8,8,9,9-Tetramethyl-3-oxo-1-phenyl-2,7-dioxa-4-aza-8-siladecane-5-carboxylate (4). *N*-Carbobenzyloxy-L-serine methyl ester (4.0 g, 16 mmol) and imidazole (1.4 g, 20.8 mmol) were taken up in DMF (dry) and stirred for 10 min. *tert*-Butyldimethylsilyl chloride (3.1 g, 20.8 mmol) was added, and the reaction mixture was stirred at room temperature for 3 h. The solvent was evaporated, and the obtained residue was purified by column chromatography using ethyl acetate/hexane (1:9) to obtain the pure product **4** as colorless oil (5.3 g, 92%). ^{1}H NMR (400 MHz, $CDCl_3$), δ (ppm): 0.02 (s, 6H); 0.86 (s, 9H); 3.76 (s, 3H); 3.85 (d, J = 9.92 Hz, 1H); 4.07 (d, J = 9.92 Hz, 1H); 4.44 (d, J = 8.65 Hz, 1H); 5.14 (s, 2H); 7.29−7.44 (m, 5H). ^{13}C NMR (100 MHz, $CDCl_3$), δ (ppm): −5.7; −5.6; 18.1; 25.6; 52.3; 55.9; 63.6; 66.9; 128.10; 128.13; 136.2; 155.9; 170.9. ESI-MS (±): calcd $C_{18}H_{29}NO_5Si$ m/z 390.2 $(M + H)^+$; found 390.2 $(M + H)^+$.

(6*R*,13*S*)-Methyl 6-(Benzyloxycarbonylamino)-2,2,3,3,17,17-hexamethyl-7,15-dioxo-4,16-dioxa-8,14-diaza-3-silaoctadecane-13-carboxylate (8). Compound **4** (3.0 g, 8.2 mmol) was dissolved in 15 mL of THF/MeOH/H_2O (3:2:2), and LiOH (0.3 g, 12.3 mmol) was added. The reaction mixture was stirred for 3 h, and the reaction completion was monitored by ESI-MS. The pH of the solution was decreased to 7 by the addition of 3 N HCl. The solvent was evaporated, and the crude product (**5**) obtained was dried under vacuum. This was redissolved in 5 mL of DMF (dry), and compound **7** (4.2 g, 10.7 mmol), NMM (2.5 mL, 23.5 mmol), and HOBt (1.7 g, 12.8 mmol) were also added under N_2. The reaction mixture was heated at 60 °C for 1 h, and EDC (12.84 mmol, 2.5 g) was added and stirred overnight. DMF was evaporated, and the residue was redissolved in $CHCl_3$ (50 mL) and extracted with water (3 × 25 mL). The collected organic layer was dried with anhydrous Na_2SO_4 and evaporated under reduced pressure. The residue obtained was purified by column chromatography using 15−20% ethyl acetate in hexane as the solvent mixture to obtain the **8** (0.35 g, 62%). ^{1}H NMR (400 MHz, $CDCl_3$), δ (ppm): 0.00 (s, 6H); 0.82 (s, 9H); 1.25−1.32 (m, 2H); 1.38 (s, 9H); 1.41−1.48 (m, 2H); 1.51−1.63 (m, 1H); 1.66−1.78 (m, 1H); 3.07−3.27 (m, 2H); 3.59 (dd, J = 7.12, 9.66 Hz, 1H); 3.65 (s, 3H); 3.94 (dd, J = 3.56 Hz, 1H); 4.06−4.26 (m, 2H); 5.05 (s, 2H); 5.71 (br. s., 1H); 6.59 (br. s., 1H); 7.18−7.38 (m, 5H). ^{13}C NMR (100 MHz, $CDCl_3$), δ (ppm): −5.7; 17.9; 22.4; 25.6; 28.1; 28.9; 31.9; 28.9; 52.0; 53.1; 55.7; 63.1; 66.8; 79.6; 135.9; 155.3; 155.9; 169.9; 173.0. ESI-HRMS (+): calcd $C_{29}H_{49}N_3O_8Si$ m/z 618.3181 $(M + Na)^+$; found 618.3181 $(M + Na)^+$.

(*S*)-Methyl 6-((*R*)-2-(Benzyloxycarbonylamino)-3-hydroxypropanamido)-2-(*tert*-butoxycarbonylamino)hexanoate (9). Compound **8** (2.5 g, 4.2 mmol) was dissolved in 10 mL of THF/TBAF (1:1), and the reaction mixture was stirred for 4 h. The solvents were evaporated, and the obtained residue was washed with water (2 × 100 mL), saturated $NaHCO_3$ (100 mL), and brine (100 mL), respectively. The collected organic layer was dried under anhydrous $NaSO_4$ and evaporated under reduced pressure. The obtained crude product was purified by column chromatography using 20−30% ethylaceate in hexane to obtain the **9** (1.6 g, 80%). ^{1}H NMR (400 MHz, $CDCl_3$), δ (ppm): 1.29−1.36 (m, 2H); 1.41 (s, 9H); 1.53−1.69 (m, 2H); 1.68−1.79 (m, 2H); 3.10−3.33 (m, 2H); 3.61−3.75 (m, 4H); 3.94−4.07 (m, 1H); 4.22 (br. s., 2H); 5.10 (s, 2H); 7.29−7.36 (m, 5H). ^{13}C NMR (100 MHz, $CDCl_3$), δ (ppm): 22.3; 28.2; 28.6; 31.8; 38.8; 52.2; 53.2; 54.8; 55.8; 62.6; 67.1; 79.9; 127.9; 128.2; 128.4; 135.9; 155.5; 156.6; 170.8; 173.3.

(6*S*,13*R*)-Methyl 13-(Benzyloxycarbonylamino)-2,2,19-trimethyl-4,12,16-trioxo-3,15,17-trioxa-5,11-diazaicosane-6-carboxylate (10). Compound **9** (1.0 g, 2.1 mmol) was dissolved in 25 mL of pyridine (0.4 mL, 4.6 mmol) containing CH_2Cl_2 and kept in acetone bath. Isobutyl chloroformate (0.55 mL, 4.2 mmol) was dissolved in 5 mL of CH_2Cl_2 and added slowly to the reaction mixture. The reaction was stirred at room temperature for 4 h. The formed crude product was extracted with water (3 × 50 mL), saturated $NaHCO_3$ (2 × 50 mL), and brine (50 mL). The organic layer was dried under Na_2SO_4 and evaporated under reduced pressure. The residue was purified by column chromatography using 15−20% ethyl acetate in hexane to obtain the pure product **10** (0.72 g, 60%). ^{1}H NMR (400 MHz, $CDCl_3$), δ (ppm): 0.92 (d, J = 6.61 Hz, 6H); 1.29−1.38 (m, 2H); 1.41 (s, 9H); 1.45−1.54 (m, 2H); 1.54−1.68 (m, 1H); 1.68−1.84 (m, 1H); 1.87−2.00 (m, 1H); 3.11−3.33 (m, 2H); 3.71 (s, 3H); 3.89 (d, J = 6.61 Hz, 2H); 4.18−4.27 (m, 1H); 4.27−4.37 (m, 1H); 4.42−4.56 (m, 2H); 5.11 (s, 2H); 7.28−7.40 (m, 5H). ^{13}C NMR (100 MHz, $CDCl_3$), δ (ppm): 18.4; 21.9; 27.3; 27.9; 28.4; 29.3; 31.6; 38.7; 51.8; 52.8; 53.6; 66.6; 66.9; 74.1; 79.5; 127.7; 127.9; 128.1; 135.5; 154.5; 155.1; 155.8; 168.1; 172.9. ESI-HRMS (+): calcd $C_{24}H_{43}N_3O_{10}$ m/z 620.2580 $(M + K)^+$; found 620.2579 $(M + K)^+$.

(6*S*,13*R*)-Methyl 13-Amino-2,2,19-trimethyl-4,12,16-trioxo-3,15,17-trioxa-5,11-diazaicosane-6-carboxylate (11). Compound **10** (0.5 g, 0.86 mmol), 10% Pd−C (0.05 g, w/w), and H_2 (50 psi) in MeOH (10 mL) was stirred for 5 h in a Parr apparatus. The reaction mixture was filtered, and the solvent was evaporated under vacuum to obtain **11** in quantitative yields, which was used as such without further purification. ^{1}H NMR (400 MHz, $CDCl_3$), δ (ppm): 0.85 (d, J = 6.10 Hz, 6H); 1.32−1.39 (m, 12H); 1.44−1.54 (m, 2H); 1.56−1.67 (m, 2H); 1.83−1.93 (m, 1H); 3.06−3.32 (m, 2H); 3.64 (s, 3H); 3.84 (d, J = 5.85 Hz, 2H); 4.09−4.32 (m, 1H); 4.32−4.70 (m, 2H). ^{13}C NMR (100 MHz, $CDCl_3$), δ (ppm): 20.0; 23.8; 28.8; 29.48; 28.5; 30.8; 33.1; 33.3; 40.5; 43.1; 53.4; 54.0; 54.3; 54.6; 67.7; 75.8; 80.5; 80.9; 155.9; 156.3; 156.8; 168.1; 174.7; 177.2. ESI-HRMS (+): calcd $C_{20}H_{37}N_3O_8$ m/z 470.2472 $(M + Na)^+$; found 470.2470 $(M + Na)^+$.

(*R*)-2-Amino-6-((*R*)-3-hydroxy-2-(5-((3a*S*,4*S*,6a*R*)-2-oxohexahydro-1*H*-thieno[3,4-*d*]imidazol-4-yl)pentanamido)propanamido)hexanoic Acid (Serine-biocytin, L_2). Compound **11** (0.14 g, 0.3 mmol) was dissolved in 4 mL of DMF (dry). D-Biotin (0.95 g, 0.4 mmol) and DIPEA (0.14 mL, 0.7 mmol) were added under N_2. The reaction mixture was stirred at room temperature for 1 h under N_2. HATU (0.18 g, 0.4 mmol) was then added, and the contents were stirred

DOI: 10.1021/cn900010d | ACS Chem. Neurosci. (2010), 1, 129–138

overnight. The reaction was monitored by ESI-MS. The solvent was evaporated, and the obtained residue was redissolved in 10 mL of THF/MeOH/H_2O (3:2:2), and LiOH (0.4 mmol, 0.011 g) was added. The reaction mixture was stirred at room temperature for 3 h, and finally TFA (10 mL) was added. This reaction was again stirred for another 3 h. The solvent was evaporated, and the obtained residue was purified by RP-HPLC to obtain the final tracer **L_2** (0.03 g, 24%). ^{1}H NMR (400 MHz, D_2O), δ ppm: 1.28−1.44 (m, 4H); 1.46−1.57 (m, 3H); 1.57−1.74 (m, 3H); 1.75−1.92 (m, 2H); 2.32 (t, J = 7.38 Hz, 2H); 2.96 (dd, J = 5.09 Hz, 2H); 3.12−3.26 (m, 2H); 3.27−3.35 (m, 1H); 3.70 (t, J = 6.61, 5.60 Hz, 1H); 3.79 (d, J = 5.60 Hz, 2H); 4.31 (t, J = 5.59 Hz, 1H); 4.39 (dd, J = 4.58 Hz, 1H); 4.57 (dd, J = 4.83 Hz, 1H). ^{13}C NMR (100 MHz, D_2O), δ ppm: 24.6; 27.8; 30.5; 30.7; 30.9; 32.9; 38.0; 41.85; 42.6; 57.4; 58.2; 63.2; 64.0; 64.9; 168.2; 174.6; 177.4; 180.0. ESI-HRMS (+): calcd $C_{19}H_{33}N_5O_6Si$ m/z 460.2224 $(M + H)^+$; found 460.2225 $(M + H)^+$.

Acknowledgment

The authors thank Prof. Dr. Klaus Albert and Prof. Dr. Martin E. Maier, Department of Organic Chemistry, University of Tübingen, for helpful discussions and providing access to the analytical facilities. The authors thank Michael Beyerlein for performing *in vivo* injections. Many thanks to Dr. Michaela Schweizer for valuable advice concerning histological processing of biocytin preparations.

Supporting Information Available

^{1}H and ^{13}C NMR spectra and ESI-HRMS of compounds **1**−**3**, **8**−**11**, **L_1**, and **L_2**. This material is available free of charge via the Internet at http://pubs.acs.org.

Author Information

Corresponding Author

* To whom correspondence should be addressed. S.C.: tel +34 91 5854445, fax +34 91 5854401, e-mail scanals@umh.es. A.M.: tel +49 7071 601651, fax +49 7071 601652, e-mail anurag.mishra@tuebingen.mpg.de.

Present Addresses

‡ Present address: Department of Chemistry, Durham University, South Road, Durham DH1 3LE, U.K.

⊥ Present address: Instituto de Neurociencias CSIC-UMH, Campus de San Juan, San Juan de Alicante 03550, Spain.

Funding Sources

This work was supported by the Max-Planck Society and the Hertie Foundation. S.C. was supported by the Human Frontiers Science Program Organization.

References

1. King, M. A., Louis, P. M., Hunter, B. E., and Walker, D. W. (1989) Biocytin: A versatile anterograde neuroanatomical tract-tracing alternative. *Brain Res. 497* (2), 361–367.

2. Lapper, S. R., and Bolam, J. P. (1991) The anterograde and retrograde transport of neurobiotin in the central nervous system of the rat: Comparison with biocytin. *J. Neurosci. Methods 39* (2), 163–174.

3. Kobbert, C., Apps, R., Bechmann, I., Lanciego, J. L., Mey, J., and Thanos, S. (2000) Current concepts in neuroanatomical tracing. *Prog. Neurobiol. 62* (4), 327–351.

4. Izzo, P. N. (1991) A note on the use of biocytin in anterograde tracing studies in the central nervous system: Application at both light and electron microscopic level. *J. Neurosci. Methods 36* (2−3), 155–166.

5. Horikawa, K., and Armstrong, W. E. (1988) A versatile means of intracellular labeling: Injection of biocytin and its detection with avidin conjugates. *J. Neurosci. Methods 25* (1), 1–11.

6. Kita, H., and Armstrong, W. (1991) A biotin-containing compound *N*-(2-aminoethyl)biotinamide for intracellular labeling and neuronal tracing studies: Comparison with biocytin. *J. Neurosci. Methods 37* (2), 141–150.

7. Chevalier, G., Deniau, J. M., and Menetrey, A. (1992) Evidence that biocytin is taken up by axons. *Neurosci. Lett. 140* (2), 197–199.

8. Baur, B., Suormala, T., and Baumgartner, E. R. (2002) Biocytin and biotin uptake into NB2a neuroblastoma and C6 astrocytoma cells. *Brain Res. 925* (2), 111–121.

9. Chang, S. L., LoTurco, J. J., and Nisenbaum, L. K. (2000) In vitro biocytin injection into perinatal mouse brain: A method for tract tracing in developing tissue. *J. Neurosci. Methods 97* (1), 1–6.

10. Wirsig-Wiechmann, C. R. (1994) Biocytin: A neuronal tracer compatible with rapid decalcification procedures. *J. Neurosci. Methods 51*, 213–216.

11. Xue, H.-G., Yang, C.-Y., and Ito, H. (2004) The anterograde and retrograde axonal transport of biotinylated dextran amine and biocytin in the nervous system of teleosts. *Brain Res. Protoc. 13*, 106–114.

12. Weiss, P., and Hiscoe, H. B. (1948) Experiments on the mechanism of nerve growth. *J. Exp. Zool. 107* (3), 315–395.

13. Baizer, J. S., Ungerleider, L. G., and Desimone, R. (1991) Organization of visual inputs to the inferior temporal and posterior parietal cortex in macaques. *J. Neurosci. 11* (1), 168–190.

14. Cowan, W. M., Gottlieb, D. I., Hendrickson, A. E., Price, J. L., and Woolsey, T. A. (1972) The autoradiographic demonstration of axonal connections in the central nervous system. *Brain Res. 37* (1), 21–51.

15. Saint-Cyr, J. A., Ungerleider, L. G., and Desimone, R. (1990) Organization of visual cortical inputs to the striatum and subsequent outputs to the pallido-nigral complex in the monkey. *J. Comp. Neurol. 298* (2), 129–156.

16. Wolf, D. E., Vallant, J., Peck, R. L., and Folkers, K. (1952) *J. Am. Chem. Soc. 74*, 2002–2003.

17. Baumgartner, E. R., Suormala, T., Wick, H., Bausch, J., and Bonjour, J. P. (1985) Biotinidase deficiency: Factors responsible for the increased biotin requirement. *J. Inherited Metab. Dis. 8* (Suppl 1), 59–64.

18. Baumgartner, E. R., Suormala, T. M., Wick, H., Probst, A., Blauenstein, U., Bachmann, C., and Vest, M. (1989) Biotinidase deficiency: A cause of subacute necrotizing encephalomyelopathy (Leigh syndrome). Report of a case with lethal outcome. *Pediatr. Res. 26* (3), 260–266.

19. Hymes, J., and Wolf, B. (1996) Biotinidase and its roles in biotin metabolism. *Clin. Chim. Acta 255* (1), 1–11.

20. Axworthy, D. B.; Theodore, L. J.; Gustavson, L. M.; Reno, J. M. U.S. Patent 5,608,660, 1997.

21. Sabatino, G., Chinol, M., Paganelli, G., Papi, S., Chelli, M., Leone, G., Papini, A. M., De Luca, A., and Ginanneschi, M. (2003) A new biotin derivative-DOTA conjugate as a candidate for pretargeted diagnosis and therapy of tumors. *J. Med. Chem. 46* (14), 3170–3173.

22. Talaga, P., Benezra, C., and Stampf, J.-L. (1990) Stereochemistry of the Michael addition of lysine derivatives to α-methylene-γ-butyrolactones. *Bioorg. Chem. 18*, 199–206.

DOI: 10.1021/cn900010d | *ACS Chem. Neurosci.* (2010), *1*, 129–138